Research Article

International Journal of
Protective Structures

International Journal of Protective Structures
2023, Vol. 14(2) 168–184

DOI: 10.1177/20414196221095252
journals.sagepub.com/home/prs
SAGE

An experimental and simulated investigation into the validity of unrestricted blast wave scaling models when applied to transonic flow in complex tunnel environments

Emily M Johnson, Nick Grahl, Martin J Langenderfer, David P Doucet, Joseph Schott, Kelly Williams, Barbara Rutter and Catherine E Johnson

Abstract

Since the inception of high explosives as an industrial tool, significant efforts have been made to understand the flow of energy from an explosive into its surroundings to maximize work produced while minimizing damaging effects. Many tools have been developed over the past century, such as the Hopkinson–Cranz (H-C) Scaling Formula, to define blast wave behavior in open air. Despite these efforts, the complexity of wave dynamics has rendered blast wave prediction difficult under confinement, where the wave interacts with reflective surfaces producing complex time-pressure waveforms. This paper implements two methods to better understand blast overpressure propagation in a confined tunnel environment and establish whether scaled tests can be performed comparatively to costly full-scale experiments. Time–pressure waveforms were predicted using both a 1:10 scaled model and three-dimensional air blast simulations conducted in Ansys Autodyn. A comparison of the reduced scale model simulation with a full-scale blast simulation resulted in self-similar overpressure waveforms when employing the H-C scaling model. Experimental overpressure waveforms showed a high level of correlation between the reduced scale model and simulations. Additionally, peak overpressure, duration, and impulse values were found to match within tolerances that are highly promising for applying this methodology in future applications. Using this validated relationship, the simulated model and reduced scale tests were used to predict an overpressure waveform in a full-scale underground mine opening to within 2.12%, 2.91%, and 7.84% for peak overpressure, time of arrival, and impulse, respectively. This paper demonstrates the effectiveness of scaled, blast models when predicting blast wave parameters in a confined environment.

Keywords

Complex waveform scaling, analytical blast modeling, Hopkinson–Cranz, scaled distance

Mining and Explosives Engineering, Missouri University of Science and Technology, Rolla, MO, USA

Corresponding author:
Catherine Johnson, Mining and Explosives Engineering, Missouri University of Science and Technology, 290 McNutt Hall, 1400 N Bishop Ave, Rolla, MO 65409-0001, USA.
Email: catherine.johnson@mst.edu

Introduction

Explosives have played a key role in the mining and defense industries for centuries (Cooper, 1937; Damnenderg, 1970; Johnson, 2010; Van Gelder Hugo Schlatter, 1928). In these professions, explosives are deliberately used in confined spaces to expedite basic processes such as mine blasting or tactical breaching (Langenderfer et al., 2021; Rutter and Johnson, 2017). In the chemical and manufacturing industries, the risk of explosion during an industrial accident presents a risk for personal and surrounding structures. As an integral part of the daily lives of workers in these fields, it has become imperative to implement safeguards to mitigate the consequences of an explosive event through blast resistant design. The effectiveness of these measures is limited by the complexity of the environment exposed to an explosion and the current knowledge of how blast waves flow through it.

While extensive work has been done to understand blast wave behavior in open air environments, significantly less exists to define the flow of an explosive blast in an environment that does not allow the shock to expand without bounds or encountering reflective obstacles (Baker et al., 1991; Cranz, 1926; Dewey, 2010, 2015; Hopkinson, 1915; Karlos et al., 2016; Prasanna Kumar et al., 2018; Seldov, 1946). The ability to predict blast wave behavior in confined environments would introduce a new avenue to inform blast resistant design for industrial processes.

A blast wave is a high-pressure disturbance that propagates into the surrounding environment at supersonic speeds (Cooper, 1937; Dewey, 2010, 2015; Karlos et al., 2016; Seldov, 1946). A blast wave can compromise the structural integrity of a building or mine, severely damage equipment and threaten the lives of personnel (Ethridge et al., 1984; Remmenikov, 2005; Ripley et al., 2016; Sherkar and Whittaker, 2010). Blast waves result from the rapid production of energy and gas during the detonation of an explosive (Cooper, 1937; Swisdak, 1975; Prasanna Kumar et al., 2018). The blast wave is characterized by an instantaneous spike in pressure at its front and trailed by a pressure region exponentially decaying in magnitude (Cooper, 1937; Chandra et al., 2012; Dewey, 2010; Karlos et al., 2016; Seldov, 1946; Swisdak, 1975). Unobstructed, the surface area of the wave front would gradually increase as the wave propagates outward, dampening the peak pressure by spreading the surface energy of the wave until it is no longer significantly greater than that of the ambient environment (Cooper, 1937; Dewey, 2010, 2015; Karlos et al., 2016; Swisdak, 1975). The magnitude of the pressure experienced at a set location from the point of origin is proportional to the time at which the pressure wave arrives after the explosion. Additionally, the pressure behind the wave decays to below ambient pressure before dampening sinusoidally back to ambient conditions (Cooper, 1937; Chandra et al., 2012; Dewey, 2010; Seldov, 1946). The change in pressure of the blast wave over time is defined as the impulse or transfer of momentum over the blast region (Cooper, 1937). This idealized blast pressure waveform is called a Friedlander waveform (Dewey, 2010, 2015; Seldov, 1946; Sochet, 2018). Each waveform is characterized by these critical blast parameters: peak overpressure, impulse, and time of arrival.

Several tools have been developed to facilitate the prediction of the critical blast parameters in an open-air blast environment (Chandra et al., 2012; Dewey, 2015; Karlos et al., 2016; Sherkar and Whittaker, 2010). Conventional Weapons Effects Program (CONWEP) and Kingery–Bulmash are examples of experimentally validated tools for predicting the overpressure and impulse produced by a spherical free air or hemispherical surface detonation, both of which produce an idealized Friedlander waveform (Karlos et al., 2016). These tools determine blast parameters for a range of distances and explosive masses by scaling the distance from the charge to a unit explosive mass using the Hopkinson–Cranz (H-C) scaling formula (Baker et al., 1991; Cranz, 1926; Hopkinson, 1915; Karlos et al., 2016).

In an unconfined environment, the H-C scaling formula, also known as the scaled distance formula, defines the criteria for determining the location at which the pressure produced by an explosive charge will be equal to that of another charge of different size (Baker et al., 1991; Cooper, 1937; Cranz, 1926; Hopkinson, 1915). If the two charges are made of the same explosive material and have the same shape, the scaling law written in equation (1) can be used to find the distance from the center of each charge, R, at which the same blast over-pressure will be measured (Baker et al., 1991; Cooper, 1937; Cranz, 1926; Hopkinson, 1915). When the weight, W, of each charge is known, the scaled distance factor, Z, is assumed to be the same for both charges and a relationship between the R of each charge is defined as

$$Z = \frac{R}{\sqrt[3]{W}} \tag{1}$$

$$\frac{R_1}{R_2} = \sqrt[3]{\frac{W_1}{W_2}} \tag{2}$$

The time between initiation and the time of arrival of the blast wave is proportionally dependent on the radial distance from the center of the charge out to the point of interest, R. This means the time it takes the blast front to reach R_1 in the full-scale system differs from the time it takes to reach R_2 in the small-scale system. The times are proportionally related by a scaling factor defined by a ratio of their radial distance from the charge, R_1:R_2. This becomes important when comparing results from scaled models.

The time elapsed from a small-scale system can be multiplied by the scaling factor to yield impulse and duration measurements equal to the corresponding full-scale model. In this study, a scaling factor of 10 is used, which has been applied to all small-scale time measurements, including scaled impulse values, presented in the current research.

The H-C Scaled Distance Formula was developed from an observed relationship during open air experiments (Baker et al., 1991; Cranz, 1926; Hopkinson, 1915). Empirical data, used to produce the Kingery-Bulmash and CONWEP blast models, validated the formula for blast waves expanding in free air, but the Friedlander waveform is only observed when a blast wave expands through the air unimpeded by rigid obstacles (Dewey, 2010, 2015; Karlos et al., 2016). The current predictive tools are not validated for blast wave predictions in situations such as bombings in urban areas, explosions inside buildings, or blasts in underground mines where reflective surfaces can direct the flow of energy from the blast wave (Cullis et al., 2016; Cullis, 2001; Ethridge et al., 1984; Langenderfer et al., 2021; Remmenikov, 2005; Rutter and Johnson, 2017).

When a blast wave propagating in air encounters a rigid obstacle, such as the ground or another reflective surface, the impedance mismatch between air and the obstacle causes an increased pressure reflection back into the incoming flow of the blast wave (Apazidis and Eliasson, 2019; Ben-Dor, 2007; Cooper, 1937; Cullis, 2001; Prasanna Kumar et al., 2018). The reflected wave can exhibit overpressures between two and 13 times greater than the shock pressure of the unimpeded blast wave itself (Apazidis and Eliasson, 2019; Ben-Dor, 2007; Cooper, 1937). These reflected waves follow behind the initial wave and, due to their higher pressure,

gradually catch up and coalesce with the initial, incident blast wave (Apazidis and Eliasson, 2019; Ben-Dor, 2007; Gault et al., 2019). Extreme underestimations of maximum overpressures are a consequence of assuming the Friedlander waveform is representative of blast wave behavior in confined environments (Cullis et al., 2016; Langenderfer et al., 2021; Rutter and Johnson, 2017; Sherkar and Whittaker, 2010). Operating under this false assumption could lead to design and safety decisions that fail to account for reflected overpressures up to eight times higher than what was predicted. Further, in an open-air blast, the blast wave profile consists of both positive and negative pressure phases. However, when an explosion takes place in a confined environment, it does not give rise to negative phase until it reaches a free space where the reflection of the overpressure wave can occur. These reflections lead to a pressure-time history that does not only contain the first phase, but multiple peaks (Chaudhary et al., 2019; Gault et al., 2019).

This paper outlines the results of a series of simulated and experimental tests that indicate that the use of the H-C Scaling model in confined air blast environments may produce reasonably accurate estimates of the critical blast wave parameters when the dimensions of the environment are scaled uniformly. It proposes two methods, simulation and experimental models, for predicting and understanding how a blast wave moves through and interacts with a complex, confined environment.

Methodology

This section describes the two experimental and two simulated models used to validate the Scaled Distance Formula, (equation (1)) in a complex, confined environment. Pressure–time measurements were collected in both a small-scale tunnel environment and in a full-scale tunnel environment. A PETN based electric detonator was used to create the overpressure wave in the small-scale tunnel environment.

A 1300 gram (g) Composition C-4 (C-4) charge with a Trinitrotoluene (TNT) equivalent mass approximately 1000 times that of the detonator was initiated in the full-scale tunnel environment. Two simulations were created all with the same tunnel design and congruent dimensions.

One simulation replicated the full-scale tunnel environment in both dimensions and size of explosive charge, and another mimicked the small-scale environment. The two simulations used the same explosive material but were scaled 1:10 in size based on the H-C Scaling formula, same as the experimental tunnel environments. Table 1 provides a summary of the explosive charges used in each test, as well as their TNT equivalence.

Instrumentation

PicoCoulomB (PCB) piezoelectric pressure sensors were used in both experimental models to gather overpressure-time data along the path of the blast wave and a Hi-Techniques Synergy P Data

Table 1. Scaled distance explosive charge summary.

	Exp. Type	Shape	Weight (g)	TNT Mass equivalent (g)
Small-scale experiment	PETN	Detonator	0.9	1.49
Small-scale simulation	PETN	Spherical	1.0	1.66
Full-scale experiment	C-4	Spherical	1300	1664
Full-scale simulation	PETN	Spherical	1000	1660

1. TNT equivalence for C-4 is based on an average value for impulse and pressure and is taken as 1.28.TNT equivalence for PETN is taken as 1.66. (Headquarters, 2019) (Department of Defense, 1986).

Acquisition System (DAS) processed the data. The PCB sensors used in this test were the PCB Piezoelectric 102B15 high frequency ICP® pressure sensors, or flush mounts. The flush mounts are capable of measuring pressures up to 200 pounds per square inch (psi) with a rise time of 1microsecond (Masahiko et al., 2001; PCB Piezotronics, 2021a, 2021b; Tressler et al., 1998). The DAS has a recording frequency of 2,000,000 samples per second.

Full-scale tunnel environment

The full-scale experimental tests were conducted in Missouri S&T's Research Mine. The dolomite limestone tunnel was created by drilling and blasting, resulting in coarse walls of varying widths and heights throughout the facility; however, a rough averaged value for the cross-sectional shape is approximately 3°m by 3°m. A 1300 g ball of C4 was detonated at the far end of the initial straight section of the mine shown in Figure 1. A 102B15 PCB sensor was placed in the path of the blast wave at sensor A1 installed in a metal plate on the floor in the side on (static) sensor orientation, as shown in Figure 1.

The facility's structure is made of limestone, which does not expand under stress but can crack and break. It is not a purely reflective surface, so some of the blast was expected to be absorbed into the rock producing underground vibrations (Chinnayya et al., 2013; Kasilingam et al., 2021; Prasanna Kumar et al., 2018). The variance in height, width, and wall smoothness was expected to cause some additional shock interactions that might result in additional noise being registered by the pressure sensor. These properties were considered as possible sources of error before the results were compared to a simulation or the scaled tunnel environments.

Small-scaled tunnel environment

A scale model of the dolomite limestone tunnel, laid out in Figure 2, was created using 12.7 mm A36 steel for the floor and walls of the model and 12.7 mm polycarbonate for the ceiling. The height of the small-scale model was 304 mm which was kept constant with the simulated model. This design is a simplified representation of the full-scale underground tunnel environment and includes analysis around a pillar to increase the complexity of the waveform beyond the straight drift measurements in the full-scale tests. A pentaerythritol tetranitrate (PETN) based electric detonator was used to produce the blast wave in the small-scale model. This detonator contained approximately 0.9 g of PETN (Powder, 2020). This mass has a TNT equivalency approximately 1000 times smaller than the mass of C-4 used in the full-scale tunnel of 1300 g (Table 1). Unlike a centrally initiated spherical charge, the energy distribution from a detonator is non-uniform and is higher from the flat end than sides. Due to the orientation of the detonator, with the flat end pointed

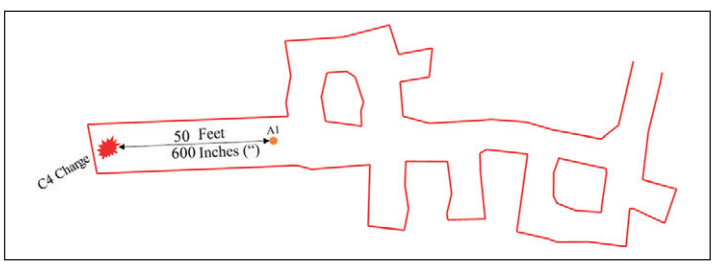

Figure 1. Full-scale environment dimensions and sensor locations.

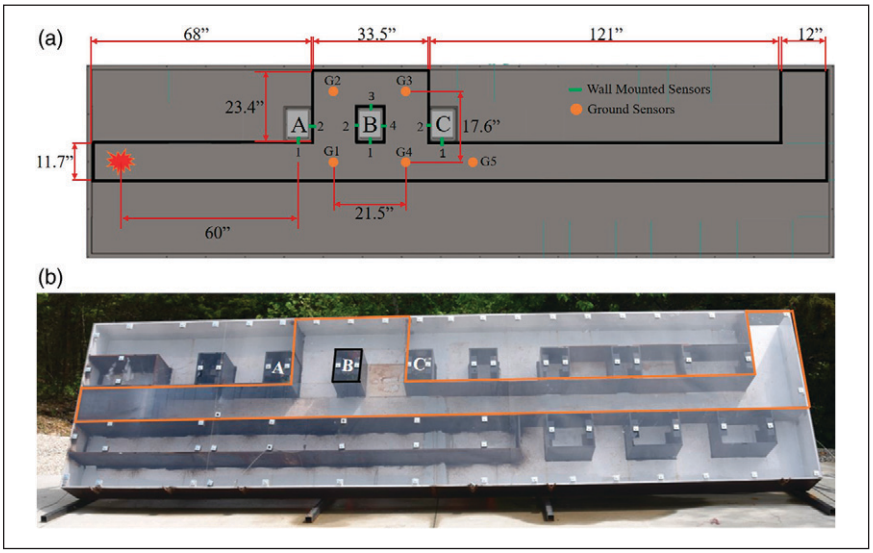

Figure 2. Scaled model dimensions and sensor locations (a); actual scaled model constructed from steel and plexiglass (b).

towards the pressure sensors, it was expected that the 0.9 g commercial detonator would be comparable to the 1 g hemispherical charge used in the simulation. Flush mount sensors were placed on the model base and walls in 13 locations, as seen in Figure 2.

All sensors were in the side on (static) orientation and flush with the model walls. The DAS was used to process and store the data from each sensor. The H-C scaling formula was used to verify that the dimensions of the model and the detonator’s distance from sensor A1 was 10 times smaller than the full-scale tunnel.

The 3D small-scale simulated model used identical dimensions to the experimental small-scale model including gauge locations with the exception that the left end of the simulated drift was shortened 304 mm lengthwise to be flush with the explosive charge. This accounted for the foam packing material used to hold the charge in place.

The design of the scaled model allowed for precision and consistency in wall width and height. Considering the ability of steel to flex under stress, the model was rigidified by welding and bolting the walls to the base of the model. Due to the different material properties of the polycarbonate ceiling, the blast wave could reflect differently to the steel model (Chinnayya et al., 2013; Prasanna Kumar et al., 2018). To reduce the flexibility of plexiglass, it was fixed with anchors visible in Figure 2(b).

Full- and small-scale simulations

Ansys/Autodyn was used to build and analyze two different simulations. This program can be used to simulate phase transitions of materials, shock wave propagation, and material response to high pressures (Chandra et al., 2012; Cullis et al., 2016; Ethridge et al., 1984). All of these are needed to accurately represent the experimental test parameters. Three-dimensional air blast simulations using Lagrange/Euler interaction were built to represent the full- and small-scale tunnel environments.

Each simulation was created with rigid Lagrangian modeled steel walls with impedance much greater than air, meaning the simulated blast wave did not lose significant energy during surface

interactions (Hong et al., 2020; Shin et al., 2014, 2015). The air was modeled using a 7.5 × 7.5 × 7.5 mm/element Euler-Flux Corrected Transport model coupled to the Lagrangian modeled tunnel geometry in order to accurately represent shock propagation and reflection through air in the tunnel geometry. The mesh size was multiplied by the geometric scaling factor of 10 for a 75 × 75 × 75 mm/element grid in the full-scale model (Hong et al., 2020). In the small-scale simulation, a hemispherical PETN charge of 1 g was modeled using a Jones Wilkins Lee product expansion in a two-dimensional axially symmetric Eulerian coordinate system (Dobratz, 1981). This model propagated to the width of the tunnel, before being remapped onto the 3 days Euler grid. In the full-scale simulation, a self-similar two-dimensional model was constructed using a 1000 g PETN charge that was remapped onto the full-scale geometry.

The two simulations were designed based on the small-scale tunnel environment that includes a pillar to alter the shock propagation from a purely straight path. Gauges were placed to collect simulated overpressure-time readings at those locations. Figure 3 shows how the simulation is an exact replica of the small-scale tunnel, with the gauges placed in the same relative locations as the pressure sensors in the small-scale tunnel shown in Figure 2. The small-scale simulation had wall dimensions equal to that of the small-scale tunnel. The full-scale simulation had dimensions 10 times larger, so the distance from the charge to A1 was equal to that in the full-scale tunnel experimental setup. The full-scale design is a 10:1 scaled up version of the small-scale simulation and small-scale tunnel. The small-scale simulation used a 1 g ball of PETN that was scaled up to 1,000g PETN for the full-scale simulation using the H-C scaling formula and to account for a lack of confinement compared to the 0.9 g detonator in the small-scale tunnel experiment.

Summary of tests

A series of small- and full-scale simulations and experiments were conducted to evaluate the use of the H-C Scaling formula in confined environments. The scale model was a 1:10 replica of the full-scale tests but included a pillar to redirect some of the explosive energy for added complexity to the evaluation.

The simulations can be compared to validate the use of the H-C Scaling Law in complex, confined environments. The experimental results from the full- and small-scale tunnel experiments can be compared to verify the use of scaled models to predict the blast behavior. Lastly, the simulation results can be compared to the experimental results to justify the use of simulation as a prediction technique.

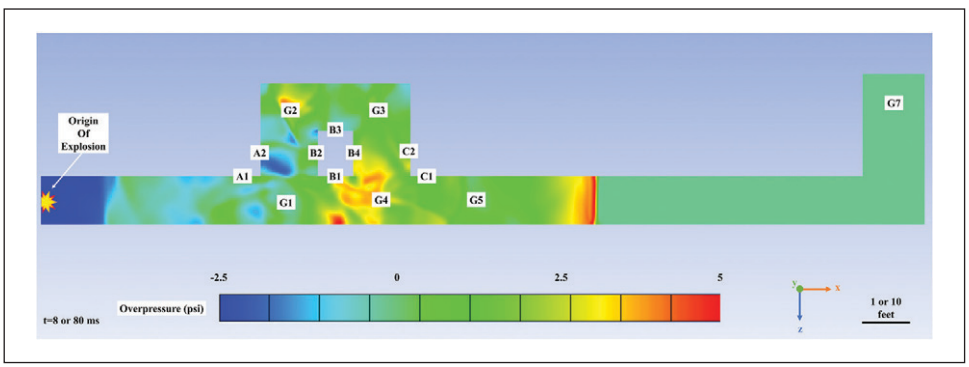

Figure 3. Design for all simulations showing gauge locations.

Results and analysis

This section compares the overpressure waveforms observed at three locations labeled in Figure 2(a) as A1, B2, and G3. These sensors were chosen to demonstrate unique complex pressure wave properties during the straight tunnel, on the back of the pillar, and on the ground behind the pillar. Gauge A1 is located at the end of a rectangular straight tunnel wall. B2 is in on a pillar wall located along the first bend away from the main straight path. G3 was placed on the floor in the far back corner behind the pillar. The data from these sensors is examined in the results section because of their unique position relative to the blast wave source and reflective surfaces. The other results can be viewed in the Supplementary Information.

The full-scale and small-scale simulations were compared to validate the H-C scaling formula in relating overpressure waves in complex confined environments. Similarity is then drawn between the full- and small-scale simulations and the data collected from the initiation of the electronic detonator in the small-scale tunnel experiment to demonstrate the accuracy of simulation in predicting experimental results. Lastly, the data collected at A1 in the full-scale tunnel experiment was compared to both of the simulations and to the small-scale tunnel experiment in an effort to validate the use of reduced-scale models to represent full scale tunnel environments (Table 2).

Full-scale simulation to small-scale simulation

Figure 4 shows selected images of the blast wave propagating through the around pillar section of the tunnel opening in the full-scale simulation from the 1000 g PETN charge.

Initially the expanding blast wave in the straight section of the tunnel reflects off the surrounding walls creating a coalescing incident wave at the A1 gauge with a peak overpressure 13.08 psi and impulse over the initial positive phase of 69.17 psi*milliseconds (ms).

At approximately 27 ms, the blast wave begins expanding into the first three-way intersection creating a dead zone of pressure immediately outside the 90-degree bend as shown in Figure 4(a).

The expansion of the blast wave into the intersection in Figure 4(b) rapidly reduces the peak overpressure of the wave to less than three psi until the wave reaches and reflects off the pillar creating a reflected wave at the B2 sensor with a peak overpressure of 8.72 psi and a significantly reduced positive phase impulse of 48.75 psi*ms due to the splitting of the incident wave at the intersection. By 60 ms the air overpressure has dropped to less than the entry level eardrum rupture threshold at five psi throughout most of the model as shown in Figure 4(c). The convergence and

Table 2. Listed measured values from small- and full-scale simulations and experiments.

Measured value	Gauge	Small-scale sim	Full-scale sim	Small-scale tunnel	Full-scale tunnel
Time of arrival (ms)	A1	24.71	24.51	25.31	25.03
	B2	37.65	37.40	37.52	-
	G3	52.59	52.31	52.05	-
Peak overpressure (psi)	A1	12.67	13.08	14.05	13.04
	B2	8.44	8.72	8.54	-
	G3	6.03	6.24	7.89	-
Positive phase impulse (psi*ms)	A1	67.16	69.17	76.84	72.49
	B2	47.32	48.75	50.64	-
	G3	96.45	99.51	103.28	-

Note that time values for small-scale tests have been increased by a factor of 10.

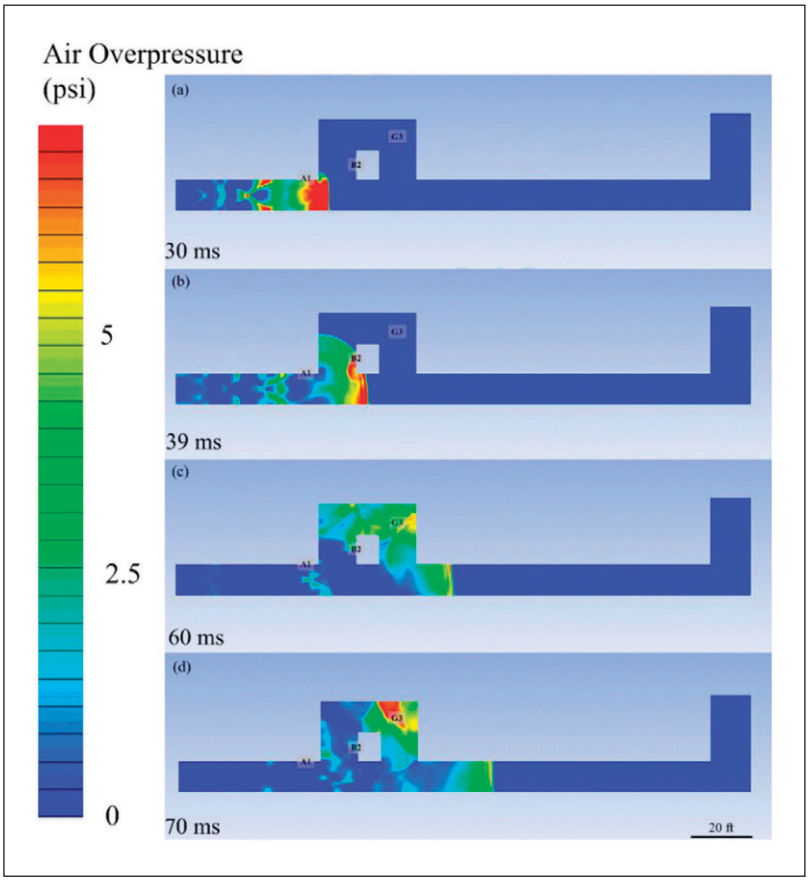

Figure 4. Simulated fringe plot of the blast wave propagating through the around pillar section of the full-scale tunnel opening showing overpressures between less than 0 psi in blue to greater than 7.25 psi in red at 30 ms (a), 39 ms (b), 60 ms (c), and 70 ms (d) after charge initiation.

stagnation of the blast waves reflecting around the pillar in the upper right region of the around pillar section of Figure 4(d) resulted in a region of prolonged pressure duration. At the G3 sensor, in this region, a lower peak overpressure of 6.24 psi is observed, however damage potential of the wave is dramatically increased by a higher impulse of 99.51 psi*ms.

The full- and small-scale simulation results were compared at three separate locations in the simulated around pillar environment. Locations of sensors B2, G3, and A1 in Figure 3 accurately represent the locations of the measurement gauges in both simulations. As discussed in the introduction, sec 1, the time required for the blast wave to travel a specified distance is reduced by ten (the designed scaling factor in these tests) in the small-scale simulation. To align the data from the small-scale simulation with that from the full-scale simulation, the time elapsed was scaled up by scaling factor, ten.

Figure 5 is a demonstration of how the H-C scaling law applies to complex environments. These were two separate simulations, run at different times. The large-scale simulation was an exact replica of the small-scale simulation, but its dimensions were scaled up tenfold and the mass of PETN detonated was increased from 1 g to 1000 g based on the H-C scaling formula.

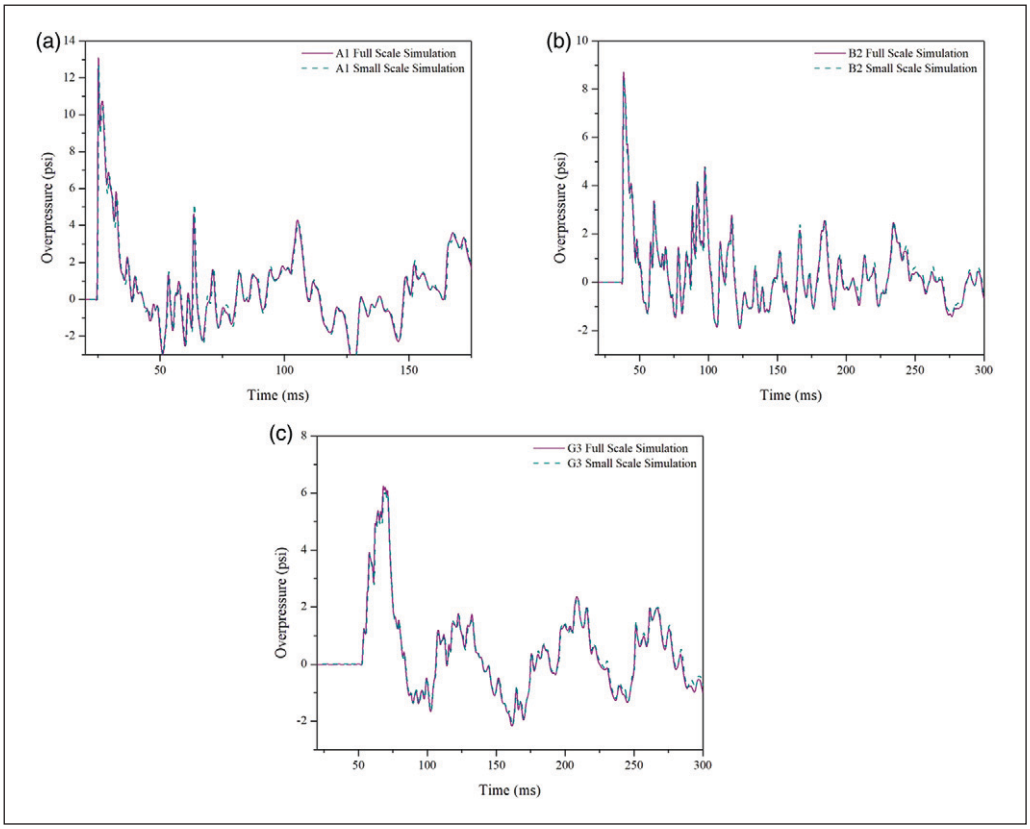

Figure 5. Full-scale versus small-scale simulation: (a) A1, (b) B2, and (c) G3. [Note that time and impulse values for small-scale tests have been increased by a factor of 10].

The similarity between the waveforms produced by the small- and large-scale simulations point to the validity of the scaling method used, despite initially being developed for open air environments. Table 3 contains the time of arrival, peak overpressure, and positive phase impulse observed in each simulation as well as the percent difference and the standard deviation between the two simulations.

The table shows the largest difference in time of arrival, peak overpressure, and positive phase impulse were observed at gauges B2, G3, and G3 respectively with percent differences of 0.68% (%), 3.40%, and 3.17%, respectively. The deviation of the blast wave observed in the full-scale simulation from that observed in the small-scale simulation is never more than 5%. These results support the use of the HC-Scaling formula to correlate blast overpressure waveforms produced in complex underground environment simulations with the tested reduced scale models.

Small-scale tunnel environment compared to full-scale simulation and small-scale simulation

The pressure data taken by Sensors A1, B2, and G3, shown in Figure 2, in the small-scale tunnel was compared to that collected in both the full and small-scale simulations. The waveforms observed at these sensors are shown in Figure 6.

Table 3. Full-scale simulation versus small-scale simulation.

Measured value	Gauge	Small-scale sim	Full-scale sim	% Difference	Std Deviation
Time of arrival (ms)	A1	24.71	24.51	0.790	0.35
	B2	37.65	37.40	0.677	0.13
	G3	52.59	52.31	0.534	0.27
Peak overpressure (psi)	A1	12.67	13.08	3.221	0.59
	B2	8.44	8.72	3.272	0.14
	G3	6.03	6.24	3.404	1.02
Positive phase impulse (psi*ms)	A1	67.16	69.17	2.991	4.23
	B2	47.32	48.75	3.027	1.67
	G3	96.45	99.51	3.168	3.42

Note that time and impulse values for small-scale tests have been increased by a factor of 10.

The blast wave time of arrival and positive phase duration are within 1.2 and 3 ms of the simulations' waveforms at all sensors. It can also be seen throughout Figure 6 that the experimental and simulated overpressure waves generally follow the same reflection pattern over time. In Table 4, the percent difference in time of arrival, peak overpressure, and positive phase impulse are listed for comparison between the small-scale model and simulations. There is a consistently larger peak overpressure and positive impulse observed in the experimental model.

The percent difference between the simulation and experimental model for these parameters remains in a range that provides valuable approximation but is significantly larger than that of the time of arrival. This variance is believed to be a result of confinement around the denotator used in the model. The similarity between the time of arrival, duration, and overall waveforms demonstrates the ability of either a 1:1 scaled simulation or a 1:10 scaled up simulation to predict blast waveforms in an around pillar tunnel environment. The likeness between the full-scale simulation and the small-scale tunnel validates the use of the H-C scaling formula in a confined environment. Investigation into TNT equivalencies of small explosives masses, especially those contained within a metal detonator, is needed.

Full-scale tunnel environment and small-scale tunnel environment compared to full-scale simulation and small-scale simulation

The results recorded by transducer A1 in the full-scale experiment are graphically compared in Figure 7 to those produced at the same location in the full-scale simulation, small-scale simulation, and the small-scale tunnel to show the effectiveness of simulation and reduced scale models to represent blast overpressure waveforms in real tunnel environments.

The overpressure waveforms produced by the simulations and in the small-scale model, shown in Figure 7, are similar to those created in the full-scale tunnel. The general waveforms seen in the simulation and small-scale model are achieved during the experimental test. For the first 45 ms the average pressure readings in the full-scale tunnel align with those in the simulation and model. After this point, while the wave peaks present themselves at the same time, the full-scale tunnel produces lower magnitude overpressure peaks. The additional overpressure spikes were expected as the result of additional noise from the experimental environment. The deviation in observed waveforms was anticipated due to the rigid and bumpy in texture and inconsistent height and width of the experimental tunnel walls.

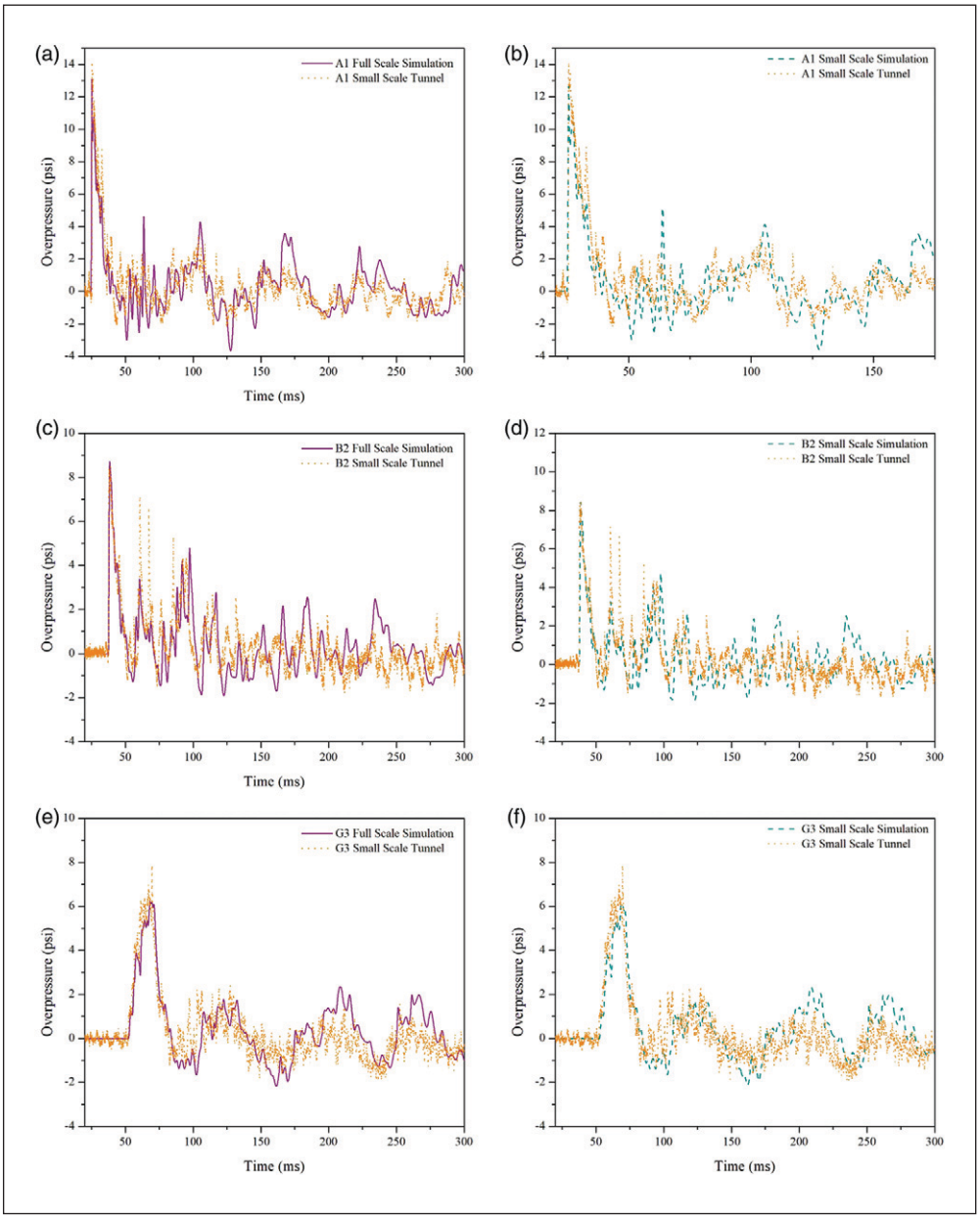

Figure 6. Overpressure-time Graph: (a), (c), (e) Full-Scale Simulation versus Small-Scale Tunnel; (b), (d), (f) Small-Scale Simulation versus Small-Scale Tunnel; (a), (b) A1; (c), (d) B2; (e), (f) G3 [Note that time and impulse values for small-scale tests have been increased by a factor of 10.].

Despite these differences, the similarity in time of arrival, peak overpressure, and positive phase impulse is considerable. Table 5 compares these values from the simulations and the small-scale model with those observed in the full-scale tunnel. The separation in these values never exceeds 10% difference.

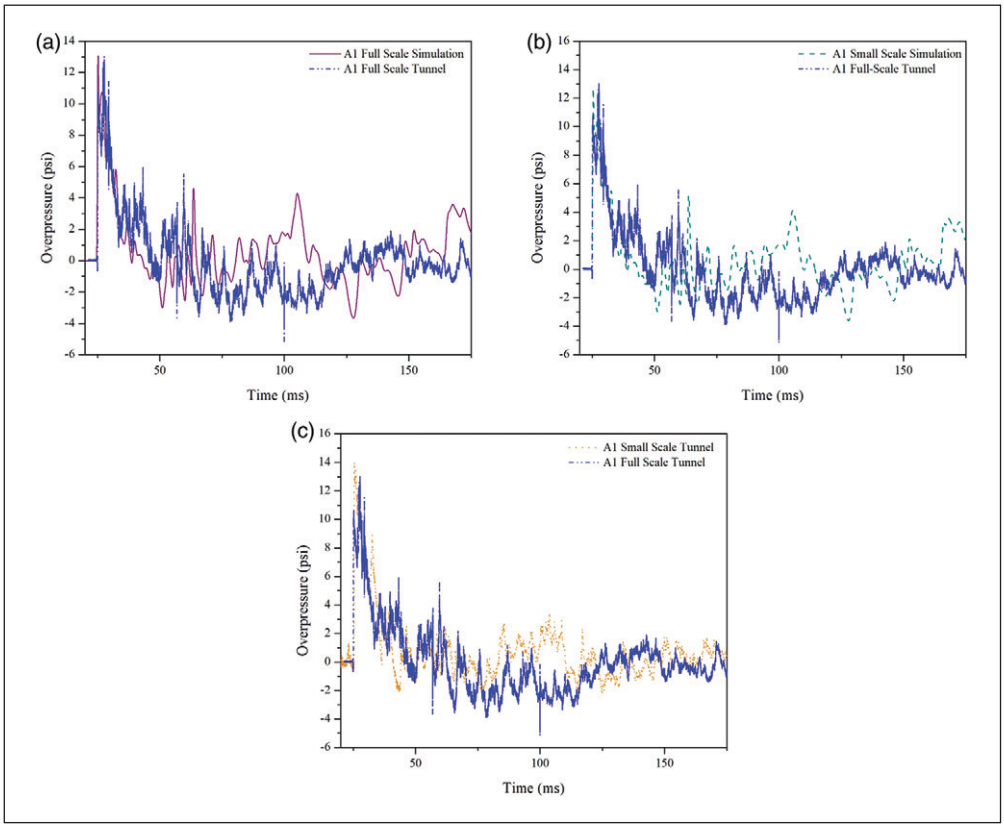

Figure 7. Overpressure-time Graph of sensor A1: (a) Full-scale simulation versus full-scale tunnel environment, (b) Small-scale simulation versus full-scale tunnel environment, and (c) Small-scale tunnel environment versus full-scale tunnel environment [Note that time and impulse values for small-scale tests have been increased by a factor of 10.].

Table 4. Small-scale tunnel environment versus simulations.

Measured value	Gauge	Small-scale tunnel	% Difference from Full Sim	% Difference from Small Sim	Std Deviation
Time of arrival (ms)	A1	25.31	3.23	2.42	0.35
	B2	37.52	0.32	0.36	0.13
	G3	52.05	0.50	1.03	0.27
Peak pressure (psi)	A1	14.05	7.43	10.89	0.59
	B2	8.54	1.97	1.23	0.14
	G3	7.89	26.40	30.70	1.02
Positive phase impulse (psi*ms)	A1	76.84	11.09	14.42	4.23
	B2	50.64	3.88	7.03	1.67
	G3	103.28	3.79	7.08	3.42

Table 5. Comparing full-scale tunnel data.

Measured value	Full-scale tunnel	% Difference Small-scale tunnel	%Difference full sim, %	% Difference small sim	Std Deviation
Time of arrival (ms)	25.03	1.08	2.12	1.31	0.35
Peak pressure (psi)	13.04	7.19	0.30	2.91	0.59
Positive phase impulse (psi*ms)	72.49	5.66	4.80	7.94	4.23

This comparison further suggests that reasonably accurate predictions can be found with the use of simulation and the H-C Scaling formula when predicting blast behavior in complex full-scale environments.

These results justified the use of simulation to represent blast wave behavior in complex tunnel and around pillar environments. They also validated the use of the H-C Scaling Formula as a tool for relating overpressure waves in confined reflective tunnel environments. The results show that the peak overpressure, impulse, and time of arrival of a waveform can be predicted in a pillar mine by a small-scale tunnel to 7.19%, 1.08%, and 5.66% accuracy, respectively, using a 1/10th scale model with H-C scaling, and within 0.3%, 2.12%, and 4.80% using a full-scale simulation.

Conclusions

This paper evaluated the effectiveness of if H-C scaling method, designed for open air environments, in a complex tunnel environment both through experiment and simulation. The peak overpressures predicted by the full-scale simulation and small-scale simulation, were within 3% of the actual observed value in the full-scale tunnel experiment. The time of arrival of the overpressure waveforms were within 2.2% of that seen in the full-scale tunnel. The difference in peak overpressure between the small-scale tunnel and large-scale tunnel tests using H-C scaling was only separated by 7.19%. The accuracy in predicting the waveform in the full-scale tunnel environment, shows the comparative strength of coupled Euler-Lagrange simulation and small-scale testing to improve understanding the behavior of blast waves in a confined environment.

The data shows that even in a confined reflective environment the H-C scaling formula can be applied to model equivalent geometrically scaled systems. Similarly, using H-C Scaling, the full-scale simulation was able to predict the observed waveforms in terms of peak overpressure and positive phase impulse in the small-scale simulation to within 3.1%. The time of arrival between the two differed by less than a percent on average. This accuracy in predicting the blast waveform in the small-scale pillar environment supports the use of simulation and the H-C scaling formula to represent blast wave behavior in complex, confined spaces. The H-C scaling formula was used to design two simulations of tunnels with around pillar complexity. The equivalence of the resulting waveforms, wave peaks, pressure durations, and impulses verified the ability of the H-C scaling formula, a formula previously only validated in open air environments, to relate blast wave behavior of different explosives in complex, confined environments. This, in turn, suggests that the use of reduced scale models to accurately depict blast wave behavior in confined environments has promising potential. This paper also displayed that a small-scale model could predict blast wave behavior in a full-sized tunnel environment with an accuracy of 4.64% of real results. The small-scale model will allow blast behavior to be studied, understood, and optimized before an explosive is detonated in a larger confined environment.

Future work

The results of the work presented in this paper lend themselves to further investigation of the use of the H-C scaling method in complex environments. Several refinements are proposed to continue to validate the use of scaling and simulations for these scenarios. First, greater standardization of explosive charges across all scales of models and simulations will help to remove any sources of error caused by confinement differences between spherical charges and the detonator used in the small-scale model presented by this research. Next, additional experimental tests can be developed, including large-scale tests that include monitoring in pillar regions, to provide additional data for analysis. Finally, materials used in the construction of small-scale models can be varied in order to investigate the impact of energy absorption within the complex environment.

Supplemental information

Additional waveforms for all sensor locations and scales for both experimental and simulation test setups can be found in the supplemental information.

Supplemental material

Supplemental Material for An experimental and simulated investigation into the validity of unrestricted blast wave scaling models when applied to transonic flow in complex tunnel environments by Emily M Johnson, Nick Grahl, Martin J Langenderfer, David P Doucet, Joseph Schott, Kelly Williams, Barbara Rutter, and Catherine Johnson in International Journal of Protective Structures

Declaration of conflicting interests

The author(s) declared no potential conflicts of interest with respect to the research, authorship, and/or publication of this article.

Funding

The author(s) disclosed receipt of the following financial support for the research, authorship, and/or publication of this article: This work was supported by the Centers for Disease Control and Prevention, specifically the National Institute for Occupational Safety and Health (project number 2017-N-18045). The Rock Mechanics and Explosives Research Center and Experimental staff were instrumental to the completion of this research by fabricating the small-scale tunnel environment experimental setup.

ORCID iD

Catherine Johnson https://orcid.org/0000-0002-0670-8179

References

Apazidis N and Eliasson V (2019) *Shock Focusing Phenomena: High Energy Density Phenomena and Dynamics of Covering Shocks*. Cham, Switzerland: Springer.

Baker WE, Westine PS and Dodge FT (1991) Scaling of air blast waves. *Fundamental Studies in Engineering* 12: 49–69.

Ben-Dor G (2007) *Shock Wave Reflection Phenomena*. Berlin: Springer.
Chandra N, Granpule S and Kleinschmit NN, et al (2012) Evolution of blast wave profiles in simulated air blast: experiment and computational modeling. *Social Work* 22: 403–415.
Chaudhary RK, Mishra S and Chakraborty T, et al (2019) Vulnerability analysis of tunnel linings under blast loading. *International Journal of Protective Structures* 10: 73–94.
Chinnayya A, Hadjadj A and Ngomo D (2013) Computaional study of detonation wave propogation in narrow channels. *Physics of Fluids* 25(3): 036101.
Cooper P (1937) *Explosives Engineering*. Wiley-VCH, inc.
Cranz KJ (1926) *Lehrubuch der Ballistik*. Berlin: Springer-Verlag.
Cullis IG, Nikiforakis N and Frankl P, et al (2016) Simulating geometrically complex blast scenarios. *Def Technol* 12: 134–146.
Cullis I (2001) Blast waves and how they interact with structures. *Journal of the Royal Army Medical Corps* 147: 16–26.
Damnenderg J (1970) *Contenporary History of Industrial Explosives in America*. ABA Pub. Co.
Department of Defense (1986) *TM 5-855-1 - Design & Analysis of Hardened Structures to Conventional Weapons Effects*. US Army (ARMY).
Dewey JM (2010) The shape of the blast wave: studies of the friedlander equation. In: 21st international symposium of military aspects of blast and shock, Israel.
Dewey JM (2015) Measurment of the physical properties of blast waves. *Experimental Methods of Shock Wave Research* 2: 53–86.
Dobratz BM (1981) *LLNL Explosives Handbook: Properties of Chemical Explosives and Explosives and Explosive Simulants*. Livermore, CA: Lawrence Livermore National Lab.
Ethridge NH, Lottero RE and Worton JD, et al (1984) *Computational and Experimental Studies of Blockage Effects in a Blast Simulator*. Adelphi, MD: US Army Ballistic Research Laboratory.
Gault K, Sochet I and Hakenholz2 L, et al (2019) Influence of the explosion center on shock wave propagation in a confined room. *Social Work* 30: 473–481.
Headquarters (2019) Department of the army. In: *TC-3-345.85-Sapper Leader Course Handbook*.
Hong X-w, Li W-b and Cheng W, et al (2020) Numerical simulation of the blast wave of a multilayer composite. *Defence Technology* 16: 96–106.
Hopkinson B (1915) UK Ordanance Board Minutes. 13565.
Johnson NG (2010) Encyclopedia britannica. In: *Explosive*. Wilmingto, DE: Britannica.
Karlos V, Solomos G and Larcher M (2016) Analysis of the blast wave decay coefficient using the Kinery-Bulmash data. *International Journal of Protective Structures* 7(3): 409–429.
Kasilingam S, Sethi M and Pelecanos L, et al (2021) Mitigation strategies of underground tunnels against blast loading. *International Journal of Protective Structures* 13: 1–24.
Langenderfer M, Williams K and Douglas A, et al (2021) An evaluation of measured and predicted air blast parameters from partially confined blast waves. *Social Work* 31: 175–192.
Masahiko I, Nagai T and Jujii Y, et al (2001) Piezoelectric pressure sensor. United States Patent US 6271621 B1.
PCB Piezotronics (2021a) Model: 102B15 ICP pressure sensor. PCB Piezotronics Inc.. Available at: https://www.pcb.com/products?m=102b15
PCB Piezotronics (2021b) Model: 137B23B ICP pressure sensor. PCB Piezotronics Inc.. Available at: https://www.pcb.com/products?m=137b23b
Powder A (2020) *RockStar Detonators Product Information Brochure*. Cleveland, OH: Austin Powder Company.
Prasanna Kumar SS, Patnaik BSV and Ramamurthi K (2018) Prediction od air blast mitigation in an array of rigid obstacles using smoothed particle hydrodynamics. *Physics of Fluids* 30(4): 046105.
Remmenikov A. (2005) Modeling blast loads on buildings in complex city geometries. *Computers and Structures* 83(27): 2197–2205.
Ripley RC, Zhang F and Cloney CT, et al (2016) A modern blast solver strategy and its urban application.
Rutter B and Johnson CE (2017) Modelling complex shock tunnel for shock interaction and transfer testing. In: 44th Annual Conference on Explosives and Blasting Technique, San Antonio, TX.

Seldov LI (1946) Propogation of strong shock waves. *Journal of Applied Mathematics and Mechanics* 10: 241–250.

Sherkar P and Whittaker AS (2010) *Modeling the Effects of Detonations of High Explosives to Inform Blast-Resistant Design*.

Shin J, Whittaker A and Aref A, et al (2014) *Air-Blast Effects on Civil Structures*. Buffalo, NY: University at Buffalo, State University of New York.

Shin J, Whittaker AS and Cormie D (2015) Incident and normally reflected overpressure and impulse for detonations of spherical high explosives in free air. *Journal of Structural Engineering* 141: 04015057.

Sochet I (2018) *Blast Effects*. New York, NY: Springer International Publishing AG.

Swisdak MM, Jr (1975) *Explosion Effects and Properties Part 1-Explosin Effects in air*. Silver Spring: White Oak Laboratory.

Tressler JF, Alkoy S and Newnham RE (1998) Piezoelectric sensors and sensor materials. *Journal of Electroceramics* 2(4): 257–272.

Van Gelder Hugo Schlatter AP (1928) History of the explosives industry in America. *Nature* 122: 765–766.